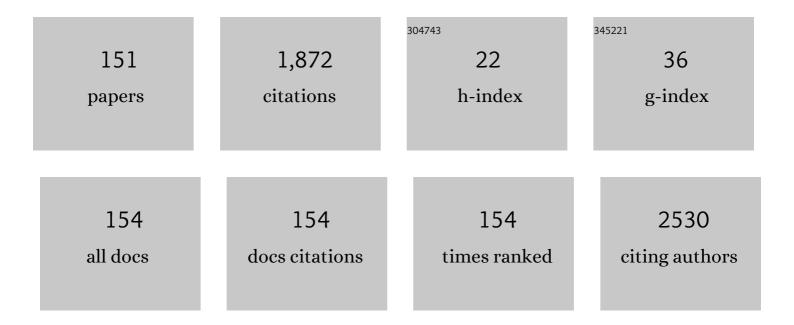
List of Publications by Year in descending order

Source: https://exaly.com/author-pdf/6506790/publications.pdf Version: 2024-02-01



#	Article	IF	CITATIONS
1	The electrical conductivity of cubic (In _{1â^'x} Ga _x) ₂ O ₃ films (x ≤0.18): native bulk point defects, Sn-doping, and the surface electron accumulation layer. Japanese Journal of Applied Physics, 2022, 61, 045502.	1.5	5
2	Direct feature extraction from two-dimensional X-ray diffraction images of semiconductor thin films for fabrication analysis. Science and Technology of Advanced Materials Methods, 2022, 2, 23-37.	1.3	1
3	Wolecular beam epitaxy of single-crystalline bixbylte <mml:math xmlns:mml="http://www.w3.org/1998/Math/MathML"> <mml:msub> <mml:mrow> <mml:mo> (</mml:mo> <mml:r< td=""><td>nsub><mn 2.4</mn </td><td>nl:mi) Tj ETQo 5</td></mml:r<></mml:mrow></mml:msub></mml:math 	nsub> <mn 2.4</mn 	nl:mi) Tj ETQo 5
4	Operando hard X-ray photoelectron spectroscopy study of buried interface chemistry of, 2022, 6, . Au/InO1.16C0.04/Al2O3/p <mml:math <br="" display="inline" xmlns:mml="http://www.w3.org/1998/Math/MathML">id="d1e383" altimg="si20.svg"><mml:math <br="" display="inline" xmlns:mml="http://www.w3.org/1998/Math/MathML">id="d1e383" altimg="si20.svg"><mml:math <br="" display="inline" xmlns:mml="http://www.w3.org/1998/Math/MathML">id="d1e383" altimg="si20.svg"><mml:math <br="" display="inline" xmlns:mml="http://www.w3.org/1998/Math/MathML">id="d1e383" altimg="si20.svg"><mml:msup><mml:mrow /><mml:mrow><mml:mco></mml:mco></mml:mrow></mml:mrow </mml:msup></mml:math>-Si stacks. Applied Surface Science, 2022, 593, 153272.</mml:math></mml:math></mml:math>	6.1	1
5	(Invited) Combinatorial Synthesis and Interface Analysis for Development of High Dielectric Constant Thin Films. ECS Transactions, 2022, 108, 61-68.	0.5	1
6	Polarity Control of an All-Sputtered Epitaxial GaN/AlN/Al Film on a Si(111) Substrate by Intermediate Oxidization. ACS Omega, 2022, 7, 19380-19387.	3.5	1
7	(Invited) Combinatorial Synthesis and Interface Analysis for Development of High Dielectric Constant Thin Films. ECS Meeting Abstracts, 2022, MA2022-01, 1070-1070.	0.0	0
8	Elobixibat, an ileal bile acid transporter inhibitor, ameliorates non-alcoholic steatohepatitis in mice. Hepatology International, 2021, 15, 392-404.	4.2	11
9	Comparison of characteristics of thin-film transistor with In ₂ O ₃ and carbon-doped In ₂ O ₃ channels by atomic layer deposition and post-metallization annealing in O ₃ . Japanese Journal of Applied Physics, 2021, 60, 030903.	1.5	6
10	Correlation between ferroelectricity and ferroelectric orthorhombic phase of HfxZr1â^'xO2 thin films using synchrotron x-ray analysis. APL Materials, 2021, 9, .	5.1	9
11	Influence of adsorbed oxygen concentration on characteristics of carbon-doped indium oxide thin-film transistors under bias stress. Japanese Journal of Applied Physics, 2021, 60, SCCM01.	1.5	3
12	Effects of Zn _x Mn _{1â^x} S buffer layer on nonpolar AlN growth on Si (100) substrate. Japanese Journal of Applied Physics, 2021, 60, SCCG02.	1.5	0
13	Effects of low temperature buffer layer on all-sputtered epitaxial GaN/AlN film on Si (111) substrate. Japanese Journal of Applied Physics, 2021, 60, SCCG03.	1.5	4
14	Accelerating two-dimensional X-ray diffraction measurement and analysis with density-based clustering for thin films. Japanese Journal of Applied Physics, 2021, 60, SCCG04.	1.5	2
15	Initial Results from High-Field-Side Transient CHI Start-Up on QUEST. Plasma and Fusion Research, 2021, 16, 2402048-2402048.	0.7	2
16	Bandgap widening and behavior of Raman-active phonon modes of cubic single-crystalline (In,Ga)2O3 alloy films. Applied Physics Letters, 2021, 119, .	3.3	3
17	Evidence-based recommender system for high-entropy alloys. Nature Computational Science, 2021, 1, 470-478.	8.0	11
18	Observation of second harmonic electron cyclotron resonance heating and current-drive transition during non-inductive plasma start-up experiment in QUEST. Plasma Physics and Controlled Fusion, 2021, 63, 105002.	2.1	4

#	Article	IF	CITATIONS
19	Development of the Material Sequencer for Automatic Various Evaluations. Journal of Surface Analysis (Online), 2021, 28, 35-45.	0.1	0
20	Valence Band Modification of a (Ga _{<i>x</i>} In _{1–<i>x</i>}) ₂ O ₃ Solid Solution System Fabricated by Combinatorial Synthesis. ACS Combinatorial Science, 2020, 22, 433-439.	3.8	10
21	Temperature and polarity dependence of electrical properties of ZnO film on pyroelectric LiNbO3single crystal. Japanese Journal of Applied Physics, 2020, 59, SIIG11.	1.5	Ο
22	Exploring the First High-Entropy Thin Film Libraries: Composition Spread-Controlled Crystalline Structure. ACS Combinatorial Science, 2020, 22, 858-866.	3.8	19
23	Dual-Heteroatom-Doped Reduced Graphene Oxide Sheets Conjoined CoNi-Based Carbide and Sulfide Nanoparticles for Efficient Oxygen Evolution Reaction. ACS Applied Materials & Interfaces, 2020, 12, 40186-40193.	8.0	25
24	Improvement in ferroelectricity and breakdown voltage of over 20-nm-thick HfxZr1â^'xO2/ZrO2 bilayer by atomic layer deposition. Applied Physics Letters, 2020, 117, .	3.3	17
25	Photoelectron spectroscopic study on electronic state of corundum In2O3 epitaxial thin film grown by mist-CVD. Japanese Journal of Applied Physics, 2020, 59, SIIG12.	1.5	4
26	Band alignment at non-polar AlN/MnS interface investigated by hard X-ray photoelectron spectroscopy. Japanese Journal of Applied Physics, 2020, 59, SIIG07.	1.5	2
27	Plasma-assisted molecular beam epitaxy of SnO(001) films: Metastability, hole transport properties, Seebeck coefficient, and effective hole mass. Physical Review Materials, 2020, 4, .	2.4	10
28	lmprovement of Ferroelectricity and Fatigue Property of Thicker Hf _x Zr _{1â^'X} O ₂ /ZrO ₂ Bi-layer. ECS Transactions, 2020, 98, 63-70.	0.5	9
29	Measurement of Dynamic Retention with Fast Ejecting System of Targeted Sample (FESTA). Plasma and Fusion Research, 2020, 15, 2402013-2402013.	0.7	1
30	Combinatorial Thin-Film Synthesis for New Nanoelectronics Materials. NIMS Monographs, 2020, , 75-87.	0.3	0
31	Switching Control of Oxide-Based Resistive Random-Access Memory by Valence State Control of Oxide. NIMS Monographs, 2020, , 69-74.	0.3	Ο
32	(Invited) Development of New High-Dielectric Constant Thin Films By Combinatorial Synthesis. ECS Transactions, 2020, 97, 61-66.	0.5	1
33	Automatic Threshold Prediction of Photoelectron Yield Spectroscopy (PYS) by Machine Learning. Vacuum and Surface Science, 2020, 63, 270-276.	0.1	2
34	Changes in Schottky Barrier Height Behavior of Pt–Ru Alloy Contacts on Single-Crystal ZnO. NIMS Monographs, 2020, , 5-26.	0.3	0
35	Surface Passivation Effect on Schottky Contact Formation of Oxide Semiconductors. NIMS Monographs, 2020, , 27-39.	0.3	0
36	Bias-Induced Interfacial Redox Reaction in Oxide-Based Resistive Random-Access Memory Structure. NIMS Monographs, 2020, , 41-67.	0.3	0

#	Article	IF	CITATIONS
37	Effects of substrate self-bias and nitrogen flow rate on non-polar AlN film growth by reactive sputtering. Japanese Journal of Applied Physics, 2019, 58, SDDG07.	1.5	8
38	Photoelectron spectroscopic study of electronic states and surface structure of an in situ cleaved In2O3 (111) single crystal. Japanese Journal of Applied Physics, 2019, 58, SDDG06.	1.5	7
39	Improvement in ferroelectricity of HfxZr1â^xO2 thin films using top- and bottom-ZrO2 nucleation layers. APL Materials, 2019, 7, .	5.1	46
40	Photoelectron spectroscopic study on electronic state and electrical properties of SnO2 single crystals. Japanese Journal of Applied Physics, 2019, 58, 080903.	1.5	6
41	Mesostructured HfO2/Al2O3 Composite Thin Films with Reduced Leakage Current for Ion-Conducting Devices. ACS Omega, 2019, 4, 14680-14687.	3.5	8
42	HFS Injection of X-Mode for EBW Conversion in QUEST. Plasma and Fusion Research, 2019, 14, 1205038-1205038.	0.7	3
43	Ferroelectricity of HfxZr1â^'xO2 thin films fabricated by 300†°C low temperature process with plasma-enhanced atomic layer deposition. Microelectronic Engineering, 2019, 215, 111013.	2.4	55
44	Gold nanoparticles anchored on mesoporous zirconia thin films for efficient catalytic oxidation of carbon monoxide at low temperatures. Microporous and Mesoporous Materials, 2019, 288, 109530.	4.4	9
45	Molecular magnetic thin films made from Ni-Co Prussian blue analogue anchored on silicon wafers. Journal of Magnetism and Magnetic Materials, 2019, 486, 165276.	2.3	10
46	Crystal growth of a MnS buffer layer for non-polar AlN on Si (100) deposited by radio frequency magnetron sputtering. Japanese Journal of Applied Physics, 2019, 58, SBBK03.	1.5	3
47	Relationship between band-offset, gate leakage current, and interface states density at SiO2/4H-SiC (000-1) interface. AIP Advances, 2019, 9, 045002.	1.3	4
48	Spectroscopic Observation of the Interface States at the SiO ₂ /4H-SiC(0001) Interface. E-Journal of Surface Science and Nanotechnology, 2019, 17, 56-60.	0.4	2
49	Photoelectroscopic Study of Mn Barrier Layer on SiO2for Si Wafer Bonding Process. , 2019, , .		0
50	Characteristics of Oxide TFT Using Carbon-Doped Ιn ₂ O ₃ Thin Film Fabricated by Low-Temperature ALD Using Ethylcyclopentadienyl Indium (Ιn-EtCp) and H ₂ O & O ₃ . ECS Transactions, 2019, 92, 3-13.	0.5	17
51	Indium oxide. , 2019, , 523-546.		4
52	Validation with Measured Data of Photoelectron Yield Spectroscopy (PYS) Threshold Using Machine Learning. Vacuum and Surface Science, 2019, 62, 504-510.	0.1	3
53	Chemical Synthesis of Multilayered Nanostructured Perovskite Thin Films with Dielectric Features for Electric Capacitors. ACS Applied Nano Materials, 2018, 1, 915-921.	5.0	11
54	Surface and bulk electronic structures of unintentionally and Mg-doped In0.7Ga0.3N epilayer by hard X-ray photoelectron spectroscopy. Journal of Applied Physics, 2018, 123, 095701.	2.5	1

ΤΑΚΑΗΙRO NAGATA

#	Article	IF	CITATIONS
55	Study of Sn and Mg doping effects on TiO ₂ /Ge stack structure by combinatorial synthesis. Japanese Journal of Applied Physics, 2018, 57, 04FJ04.	1.5	0
56	Combinatorial Thin Film Synthesis for Developments of New High Dielectric Constant Thin Film Materials. Transactions of the Materials Research Society of Japan, 2018, 43, 249-254.	0.2	1
57	Reliability of Al2O3/In-Si-O-C Thin-Film Transistors with an Al2O3 Passivation Layer under Gate-Bias Stress. ECS Transactions, 2018, 86, 135-145.	0.5	4
58	Ferroelectricity of Hf _x Zr _{1â^x} O ₂ Thin Films Fabricated Using TiN Stressor and ZrO ₂ Nucleation Techniques. ECS Transactions, 2018, 86, 31-38.	0.5	9
59	Auger Depth Profiling Analysis of HfO ₂ /Si Specimen Using an Ultra Low Angle Incidence Ion Beam. Journal of Surface Analysis (Online), 2018, 24, 192-205.	0.1	1
60	Photoelectron spectroscopic study on monolayer pentacene thin-film/polar ZnO single-crystal hybrid interface. Applied Physics Express, 2017, 10, 025702.	2.4	5
61	Hard X-Ray Photoelectron Spectroscopic Study on High-k Dielectrics Based Resistive Random Access Memory. ECS Transactions, 2017, 75, 39-47.	0.5	0
62	Crystallographic polarity effect of ZnO on thin film growth of pentacene. Japanese Journal of Applied Physics, 2017, 56, 04CJ03.	1.5	4
63	Ferroelectric-assisted gold nanoparticles array for centimeter-scale highly reproducible SERS substrates. Scientific Reports, 2017, 7, 3630.	3.3	15
64	Surface and bulk electronic structures of heavily Mg-doped InN epilayer by hard X-ray photoelectron spectroscopy. Journal of Applied Physics, 2017, 121, .	2.5	5
65	Photoelectron spectroscopic study of electronic state and surface structure of In2O3 single crystals. Applied Physics Express, 2017, 10, 011102.	2.4	9
66	Effect of Y and Mn doping into rutile type TiO2/Ge stack structure by combinatorial synthesis. Japanese Journal of Applied Physics, 2017, 56, 06GF11.	1.5	3
67	Direct Observation of the Energy Distribution of Interface States at SiO ₂ /4H-SiC Interface: Operando Hard X-ray Photoelectron Spectroscopic Study. Hyomen Kagaku, 2017, 38, 347-350.	0.0	Ο
68	Thin-film growth of (110) rutile TiO2on (100) Ge substrate by pulsed laser deposition. Japanese Journal of Applied Physics, 2016, 55, 06GG06.	1.5	2
69	Bottom-electrode effect on switching behavior and interface reaction in nanoionic-based resistive changing memory. Japanese Journal of Applied Physics, 2016, 55, 08PC03.	1.5	1
70	Interfacial charge transfer behavior of conducting polymers as contact electrode for semiconductor devices. Japanese Journal of Applied Physics, 2016, 55, 04EC10.	1.5	0
71	Screening charge localization at LiNbO3 surface with Schottky junction. Applied Physics Letters, 2016, 108, .	3.3	1
72	Contacting ZnO Individual Crystal Facets by Direct Write Lithography. ACS Applied Materials & Interfaces, 2016, 8, 23891-23898.	8.0	2

#	Article	IF	CITATIONS
73	Direct Observation of Energy Distribution of Interface States at SiO2/4H-SiC Interface. ECS Transactions, 2016, 75, 207-211.	0.5	0
74	Tooth Root Bending Stress Analysis of Pre-alloyed Sintered Steel Gears with Different Densities using FEM Model Considering Voids. Funtai Oyobi Fummatsu Yakin/Journal of the Japan Society of Powder and Powder Metallurgy, 2016, 63, 568-572.	0.2	1
75	Arbitrary cross-section SEM-cathodoluminescence imaging of growth sectors and local carrier concentrations within micro-sampled semiconductor nanorods. Nature Communications, 2016, 7, 10609.	12.8	13
76	Interface stability of electrode/Bi-containing relaxor ferroelectric oxide for high-temperature operational capacitor. Japanese Journal of Applied Physics, 2016, 55, 06GJ12.	1.5	1
77	Heteroepitaxial growth of nonpolar Cu-doped ZnO thin film on MnS-buffered (100) Si substrate. Japanese Journal of Applied Physics, 2015, 54, 06FJ10.	1.5	3
78	Band-Gap Deformation Potential and Elasticity Limit of Semiconductor Free-Standing Nanorods Characterized <i>in Situ</i> by Scanning Electron Microscope–Cathodoluminescence Nanospectroscopy. ACS Nano, 2015, 9, 2989-3001.	14.6	22
79	Altering properties of cerium oxide thin films by Rh doping. Materials Research Bulletin, 2015, 67, 5-13.	5.2	20
80	BaTiO ₃ based relaxor ferroelectric epitaxial thin-films for high-temperature operational capacitors. Japanese Journal of Applied Physics, 2015, 54, 04DH02.	1.5	9
81	Combinatorial synthesis of BaTiO3–Bi(Mg2/3Nb1/3)O3thin-films for high-temperature capacitors. Japanese Journal of Applied Physics, 2015, 54, 06FJ02.	1.5	4
82	Bias induced Cu ion migration behavior in resistive change memory structure observed by hard X-ray photoelectron spectroscopy. Japanese Journal of Applied Physics, 2015, 54, 06FG01.	1.5	3
83	Ge incorporated epitaxy of (110) rutile TiO2 on (100) Ge single crystal at low temperature by pulsed laser deposition. Thin Solid Films, 2015, 591, 105-110.	1.8	8
84	Epitaxial growth of high dielectric constant lead-free relaxor ferroelectric for high-temperature operational film capacitor. Thin Solid Films, 2015, 592, 29-33.	1.8	6
85	Interfacial Charge Transfer Behaviour of Conducting Polymers as Contact Electrode for Semiconductor Devices. , 2015, , .		0
86	Epitaxial growth of nonpolar ZnO and n-ZnO/i-ZnO/p-GaN heterostructure on Si(001) for ultraviolet light emitting diodes. Applied Physics Express, 2014, 7, 062102.	2.4	14
87	(Invited) Photoelectron Spectroscopic Study on High-k Dielectrics Based Nanoionics-Type ReRAM Structure under Bias Operation. ECS Transactions, 2014, 61, 301-310.	0.5	0
88	Photoelectron spectroscopic study on band alignment of poly(3-hexylthiophene-2,5-diyl)/polar-ZnO heterointerface. Thin Solid Films, 2014, 554, 194-198.	1.8	3
89	Resolving lateral and vertical structures by ellipsometry using wavelength range scan. Thin Solid Films, 2014, 571, 579-583.	1.8	8
90	Highly conductive epitaxial ZnO layers deposited by atomic layer deposition. Thin Solid Films, 2014, 562, 485-489.	1.8	17

ΤΑΚΑΗΙRO NAGATA

#	Article	IF	CITATIONS
91	Charge-Transfer Behavior of Conducting Polymers as Contact Electrode for Semiconductor Devices. , 2014, , .		0
92	Generalized mechanism of the resistance switching in binary-oxide-based resistive random-access memories. Physical Review B, 2013, 87, .	3.2	52
93	Combinatorial Synthesis of Cu/(TaxNb1–x)2O5 Stack Structure for Nanoionics-Type ReRAM Device. ACS Combinatorial Science, 2013, 15, 435-438.	3.8	5
94	Impact of Mg concentration on energy-band-depth profile of Mg-doped InN epilayers analyzed by hard X-ray photoelectron spectroscopy. Applied Physics Letters, 2013, 103, .	3.3	8
95	Improving the performance of inorganic-organic hybrid photovoltaic devices by uniform ordering of ZnO nanorods and near-atmospheric pressure nitrogen plasma treatment. Journal of Applied Physics, 2013, 113, 083708.	2.5	10
96	Systematic investigation of surface and bulk electronic structure of undoped In-polar InN epilayers by hard X-ray photoelectron spectroscopy. Journal of Applied Physics, 2013, 114, .	2.5	17
97	Influence of the annealing atmosphere on the structural properties of FePt thin films. Journal of Applied Physics, 2013, 114, .	2.5	22
98	Reduction of interfacial SiO2 at HfO2/Si interface with Ta2O5 cap. Journal of Applied Physics, 2013, 114, .	2.5	4
99	Nanoimprint for Fabrication of Highly Ordered Epitaxial ZnO Nanorods on Transparent Conductive Oxide Films. Applied Physics Express, 2012, 5, 095003.	2.4	12
100	Hard x-ray photoelectron spectroscopy study on band alignment at poly(3,4-ethylenedioxythiophene):poly(styrenesulfonate)/ZnO interface. Applied Physics Letters, 2012, 101, .	3.3	21
101	Electrical properties and stability of an epitaxial alumina film formed on Cu-9 at. % Al(111). Journal of Vacuum Science and Technology A: Vacuum, Surfaces and Films, 2012, 30, 021509.	2.1	2
102	Development of AlN/diamond heterojunction field effect transistors. Diamond and Related Materials, 2012, 24, 206-209.	3.9	31
103	Observation of filament formation process of Cu/HfO ₂ /Pt ReRAM structure by hard x-ray photoelectron spectroscopy under bias operation. Journal of Materials Research, 2012, 27, 869-878.	2.6	7
104	Electron transport in semiconducting SnO ₂ : Intentional bulk donors and acceptors, the interface, and the surface. Journal of Materials Research, 2012, 27, 2232-2236.	2.6	26
105	Effect of near atmospheric pressure nitrogen plasma treatment on Pt/ZnO interface. Journal of Applied Physics, 2012, 112, .	2.5	2
106	Investigations into the Impact of the Template Layer on ZnO Nanowire Arrays Made Using Low Temperature Wet Chemical Growth. Crystal Growth and Design, 2011, 11, 2515-2519.	3.0	41
107	XPS study of Sb-/In-doping and surface pinning effects on the Fermi level in SnO2 (101) thin films. Applied Physics Letters, 2011, 98, .	3.3	38
108	Depletion of the In2O3(001) and (111) surface electron accumulation by an oxygen plasma surface treatment. Applied Physics Letters, 2011, 98, .	3.3	71

ΤΑΚΑΗΙRO NAGATA

#	Article	IF	CITATIONS
109	XPS and UPS study on band alignment at Pt–Zn-terminated ZnO(0001) interface. Applied Surface Science, 2011, 258, 780-785.	6.1	34
110	New Phases of sp[sup 3]-bonded Boron Nitride Prepared by Photo-Assisted Plasma Processing Methods: The Fundamentals and Applications to Electronic Devices. , 2011, , .		0
111	Effect of UV–ozone treatment on electrical properties of PEDOT:PSS film. Organic Electronics, 2011, 12, 279-284.	2.6	77
112	Bias application hard x-ray photoelectron spectroscopy study of forming process of Cu/HfO2/Pt resistive random access memory structure. Applied Physics Letters, 2011, 99, .	3.3	56
113	Bias-application in Hard X-ray Photoelectronic Study for Advanced Materials. Hyomen Kagaku, 2011, 32, 320-324.	0.0	0
114	XPS study on band alignment at PtOâ€ŧerminated ZnO(0001) interface. Surface and Interface Analysis, 2010, 42, 1528-1531.	1.8	21
115	Schottky barrier height behavior of Pt–Ru alloy contacts on single-crystal n-ZnO. Journal of Applied Physics, 2010, 107, .	2.5	6
116	Photoinduced Phase Transformations in Boron Nitride: New Polytypic Forms of sp ³ -Bonded (6H- and 30H-) BN. Journal of Physical Chemistry C, 2010, 114, 13176-13186.	3.1	11
117	Study of the Au Schottky contact formation on oxygen plasma treated n-type SnO2 (101) thin films. Journal of Applied Physics, 2010, 107, 033707.	2.5	45
118	Interface structure and the chemical states of Pt film on polar-ZnO single crystal. Applied Physics Letters, 2009, 94, 221904.	3.3	18
119	Surface structure and chemical states of a-plane and c-plane InN films. Applied Physics Letters, 2009, 95, .	3.3	46
120	Dissipation-factor-based criterion for the validity of carrier-type identification by capacitance-voltage measurements. Applied Physics Letters, 2009, 94, 152110.	3.3	10
121	Non-Alloyed Schottky and Ohmic Contacts to As-Grown and Oxygen-Plasma Treated n-Type SnO ₂ (110) and (101) Thin Films. Applied Physics Express, 2009, 2, 106502.	2.4	31
122	Effect of Annealing on Mechanical Properties of Materials Formed by Focused Au or Si Ion-Beam-Induced Chemical Vapor Deposition Using Phenanthrene. Japanese Journal of Applied Physics, 2009, 48, 06FB03.	1.5	1
123	Highly Uniform Epitaxial ZnO Nanorod Arrays for Nanopiezotronics. Nanoscale Research Letters, 2009, 4, 699-704.	5.7	54
124	Prediction of iodide adsorption on oxides by surface complexation modeling with spectroscopic confirmation. Journal of Colloid and Interface Science, 2009, 332, 309-316.	9.4	59
125	Surface Nitridation ofc-Plane Sapphire Substrate by Near-Atmospheric Nitrogen Plasma. Japanese Journal of Applied Physics, 2009, 48, 040206.	1.5	5
126	P-type sp3-bonded BN/n-type Si heterodiode solar cell fabricated by laser–plasma synchronous CVD method. Journal Physics D: Applied Physics, 2009, 42, 225107.	2.8	6

Τακαμιγό Νάσατα

#	Article	IF	CITATIONS
127	Composition-spread thin films of pentacene and 6,13-pentacenequinone fabricated by using continuous-wave laser molecular beam epitaxy. Applied Surface Science, 2008, 254, 2336-2341.	6.1	12
128	Thermal stability of Ni silicide films on heavily doped n+ and p+ Si substrates. Microelectronic Engineering, 2008, 85, 1642-1646.	2.4	12
129	Fully engineered homoepitaxial zinc oxide nanopillar array for near-surface light wave manipulation. Applied Physics Letters, 2008, 92, 183114.	3.3	14
130	Ni silicidation on heavily doped Si substrates. , 2008, , .		0
131	Characterization of Deposited Materials Formed by Focused Ion Beam-Induced Chemical Vapor Deposition Using AuSi Alloyed Metal Source. Japanese Journal of Applied Physics, 2008, 47, 5018-5021.	1.5	2
132	Effect of Annealing on Implanted Ga of Diamond-Like Carbon Thin Films Fabricated by Focused-Ion-Beam Chemical Vapor Deposition. Japanese Journal of Applied Physics, 2008, 47, 9010-9012.	1.5	13
133	Crystal Structures of Pt–Ru Alloy Schottky Contacts on ZnO by Combinatorial Ion Beam Deposition. Japanese Journal of Applied Physics, 2007, 46, 2907-2909.	1.5	4
134	GaN Film Fabrication by Near-Atmospheric Plasma-Assisted Chemical Vapor Deposition. Japanese Journal of Applied Physics, 2007, 46, L43-L45.	1.5	4
135	Schottky metal library for ZNO-based UV photodiode fabricated by the combinatorial ion beam-assisted deposition. Applied Surface Science, 2006, 252, 2503-2506.	6.1	31
136	Composition spread metal thin film fabrication technique based on ion beam sputter deposition. Applied Surface Science, 2006, 252, 2472-2476.	6.1	15
137	Electro-optical effect in ZnO:Mn thin films prepared by Xe sputtering. Journal of Applied Physics, 2006, 99, 013509.	2.5	18
138	Low-temperature growth of GaN microcrystals from position-controlled Ga droplets arrayed by a low-energy focused ion beam system. Journal of Crystal Growth, 2005, 283, 328-331.	1.5	3
139	Effects of Single-Crystalline GaN Target on GaN Thin Films in Pulsed Laser Deposition Process. Japanese Journal of Applied Physics, 2005, 44, 7896-7900.	1.5	3
140	GaN nanostructure fabrication by focused-ion-beam-assisted chemical vapor deposition. Applied Physics Letters, 2005, 87, 013103.	3.3	12
141	The effects of Xe on an rf plasma and growth of ZnO films by rf sputtering. Journal of Applied Physics, 2004, 95, 3923-3927.	2.5	32
142	Optical propagation loss of ZnO films grown on sapphire. Journal of Applied Physics, 2004, 95, 1673-1676.	2.5	7
143	Electro-optic effect in ZnO:Mn thin films. Journal of Alloys and Compounds, 2004, 371, 157-159.	5.5	14
144	Position Controlled GaN Nano-Structures Fabricated by Low Energy Focused Ion Beam System Materials Research Society Symposia Proceedings, 2003, 792, 621.	0.1	0

#	Article	IF	CITATIONS
145	Electro-Optic Effect in Epitaxial ZnO:Mn Thin Films. Japanese Journal of Applied Physics, 2002, 41, 6916-6918.	1.5	17
146	Electro-optic property of ZnO:X (X=Li,Mg) thin films. Journal of Crystal Growth, 2002, 237-239, 533-537.	1.5	59
147	Life cycle CO 2 analysis of LNG and city gas. Applied Energy, 2001, 68, 301-319.	10.1	50
148	Ferroelectricity in Li-Doped ZnO:X Thin Films and their Application in Optical Switching Devices. Japanese Journal of Applied Physics, 2001, 40, 5615-5618.	1.5	33
149	Impact of Cu Electrode on Switching Behavior in a Cu/HfO ₂ /Pt Structure and Resultant Cu Ion Diffusion. Applied Physics Express, 0, 2, 061401.	2.4	106
150	Kerr effect microscope combined with a pulse magnet to observe high-entropy alloys fabricated using combinatorial technology. Science and Technology of Advanced Materials Methods, 0, , .	1.3	0
151	Effect of reactive gas condition on nonpolar AlN film growth on MnS/Si (100) by reactive DC sputtering. Japanese Journal of Applied Physics, 0, , .	1.5	1